Supporting Material I: Figures S1 and S2

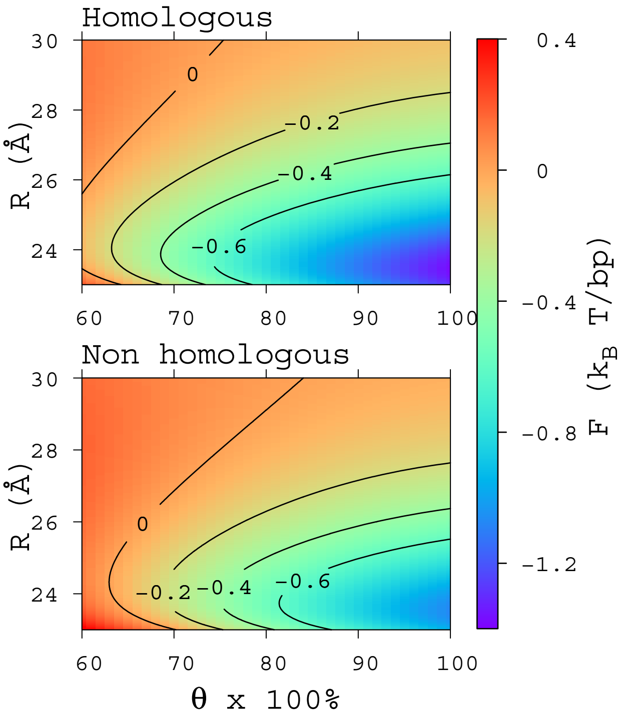

Figure S1. Optimized free energy as a function of R and *θ*. The energy contour map is given for homologous (upper panel) and non homologous (lower panel) molecules. The free energy was calculated from Eqs. (3)-(8) of the main text at a=11.2 Å, λ_D = 7 Å, f_1=0.4, and f_2=0.6.

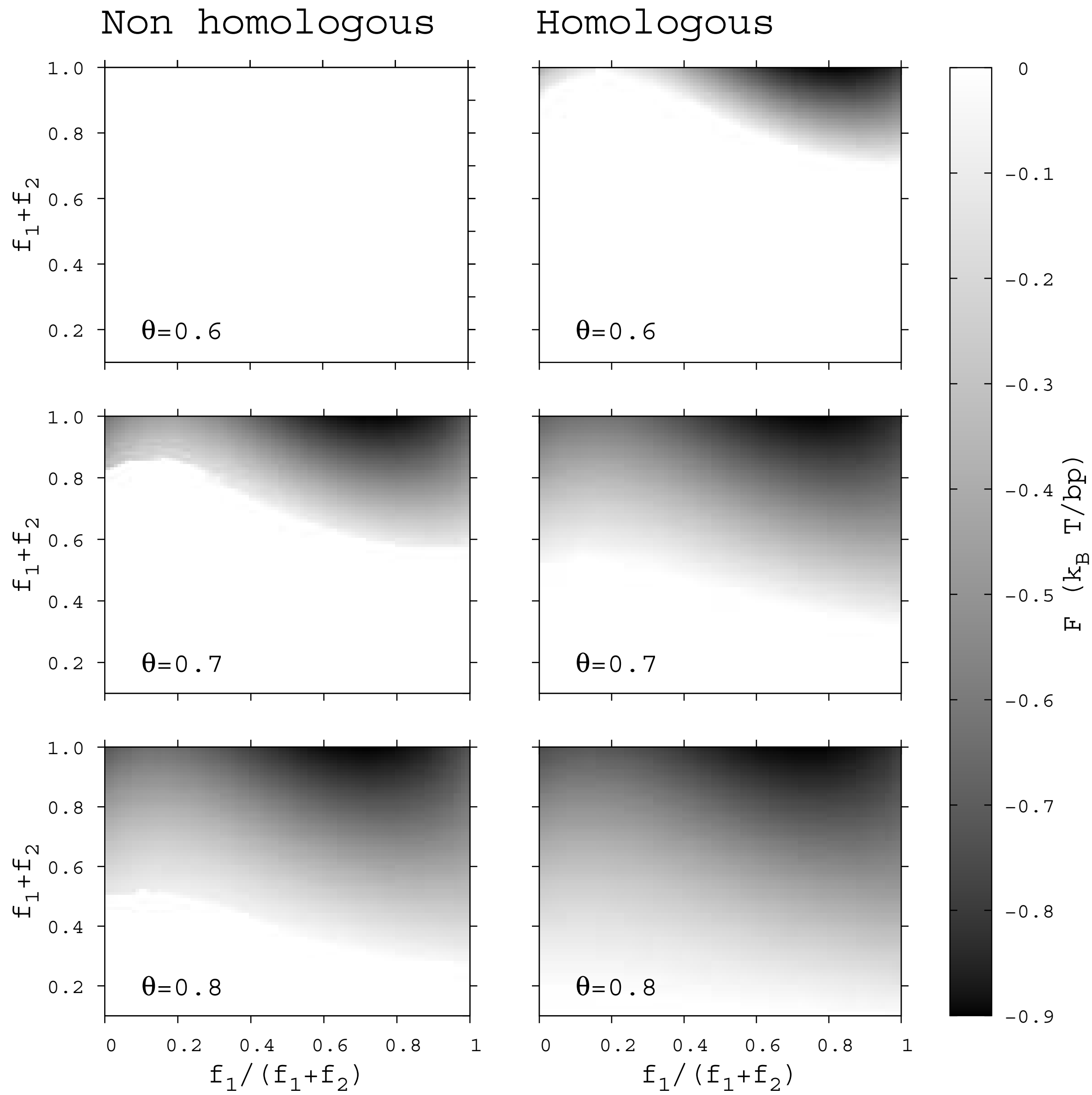

Figure S2. Pairing energy landscapes as a function of total portion of the adsorbed (condensed) counterions in the grooves ($f_1 + f_2$) and the relative weight of the minor group population, $f_1 /(f_1 + f_2)$, for the indicated values of the charge compensation parameter θ. All other parameters were the same as in Fig. 3 of the main text. Left column: nonhomologous pairs, right column: homologous pairs. The empty upper left landscape shows that pairing of nonhomologous DNA molecules is energetically unfavorable at $\theta = 0.6$ regardless of the pattern of bound counterions.

Supporting Material II: Theory of Braided Pairs of Charged Helical Molecules

In this Supporting Material we derive expressions for the electrostatic and free energy of symmetric, straight DNA braids. In Part A, we develop an electrostatic theory for ideal, symmetric braids of charged helical molecules. We begin by considering braided pairs of molecules with arbitrary patterns of discrete surface charges and then demonstrate the theory's application to ideal helical chains and double helices. In part B, we discuss effects of sequence-related and thermal fluctuations in the double helix structure and calculate the corresponding free energy of DNA braids.

To avoid disrupting the main line of the presentation, we provide clarifying auxiliary arguments in shaded boxes. We utilize the Gaussian system of units for the electrostatic equations.

A. ELECTROSTIC ENERGY

A.1 General Strategy

Our calculation of electrostatic energy of braided pairs of molecules is based on the following general ideas. We represent the energy of braid formation as

$$E_{BR}\left(R\right)=E\left(R\right)-E\left(\infty\right). \qquad \text{(S1)}$$

Here R is the braid diameter defined at the centerlines of the molecules (Fig. 2 of the main text) and

$$E\left(R\right)=\frac{1}{2}\int\varphi(\mathbf{r})\rho(\mathbf{r})d^3\mathbf{r} \qquad \text{(S2)}$$

is the energy of all fixed charges of the molecules (charge density $\rho(\mathbf{r})$) in the electrostatic potential $\varphi(\mathbf{r})$ created by these charges.

For braids immersed in an electrolyte solution, we utilize a model, in which all bound and condensed counterions within the nonlinear screening layer are treated as part of the surface charge of the molecules and contribute to $\rho(\mathbf{r})$ (1). Hereafter, we refer to these counterions as bound. We assume that the molecules have cylindrical dielectric cores with a dielectric constant much smaller than that of water. We also assume that the fixed charges and bound counterions lie at the core-water interface. Within this model, the electrostatic potential $\varphi(\mathbf{r})$ outside and at the surfaces of the dielectric cores may be calculated from the Debye-Huckel equation,

$$\Delta\varphi(\mathbf{r})-\kappa_D^2\varphi(\mathbf{r})=-\frac{4\pi}{\varepsilon}\left[\rho(\mathbf{r})+\rho^{ind}(\mathbf{r})\right], \qquad \text{(S3)}$$

in which we account for the effects of the dielectric cores on $\varphi(\mathbf{r})$ by introducing the density $\rho^{ind}(\mathbf{r})$ of induced charges at the surfaces of the cores (often referred to as "image charges"). Here ε is the dielectric constant of water and κ_D is the inverse screening (Debye) length. The density of the induced (image) charges is calculated by solving the Laplace equation for the potential inside the cores and using appropriate boundary conditions at the core-water interface (6).

From Eqs. (S2) and (S3), we find that

$$E\left(R\right)=\frac{2\pi}{\varepsilon}\sum_{\mu,\nu=1}^{2}\int d^3\mathbf{k}\frac{\left[\tilde{\rho}_\mu(\mathbf{k})+\tilde{\rho}_\mu^{ind}(\mathbf{k})\right]\tilde{\rho}_\nu(-\mathbf{k})}{k^2+\kappa_D^2} \qquad \text{(S4)}$$

where $\tilde{\rho}_\nu(\mathbf{k})$, $\tilde{\rho}_\mu(\mathbf{k})$ and $\tilde{\rho}_\mu^{ind}(\mathbf{k})$ are Fourier transforms

$$\tilde{\rho}(\mathbf{k})=\frac{1}{(2\pi)^{3/2}}\int\rho(\mathbf{r})e^{i\mathbf{k}\cdot\mathbf{r}}d^3\mathbf{r} \qquad \text{(S5)}$$

of the densities of fixed $\rho_\nu(\mathbf{r})$ and induced $\rho_\nu^{ind}(\mathbf{r})$ charges at the surface of the dielectric cores of the molecules ν and μ ($\nu,\mu = 1,2$).

To calculate the electrostatic energy, we exploit the fact that for helical charge patterns $\tilde{\rho}_\nu(\mathbf{k})$ and $\tilde{\rho}_\nu^{ind}(\mathbf{k})$ are not zero only within a limited set of $\mathbf{k}$, allowing us to calculate the integral in Eq. (S4). Specifically, we represent $\tilde{\rho}_\nu^{ind}(\mathbf{k})$ by a series of image charges (Box 1). After truncation of this series and utilizing the reciprocity of electrostatic interactions, we arrive at the following approximation (for derivation, see Box 1)

$$E_{BR}(R)=E_{1,2}(R)+E_{1,1}(R)+E_{2,2}(R) \qquad \text{(S6)}$$

where

$$E_{1,2}(R)\approx\frac{4\pi}{\varepsilon}\int d^3\mathbf{k}\frac{\left[\tilde{\rho}_1(\mathbf{k})+\tilde{\rho}_{1,1}^{(0)}(\mathbf{k})\right]\left[\tilde{\rho}_2(-\mathbf{k})+\tilde{\rho}_{2,2}^{(0)}(-\mathbf{k})\right]}{k^2+\kappa_D^2} \qquad \text{(S7)}$$

is the energy of fixed charges of molecule 2 in the electric field created by molecule 1 (which is equal to the energy of fixed charges of molecule 1 in the field created by molecule 2);

$$E_{\nu,\nu}(R)\approx\frac{2\pi}{\varepsilon}\int d^3\mathbf{k}\frac{\tilde{\rho}_{\nu,\mu}^{(1)}(\mathbf{k})\left[\tilde{\rho}_\mu(-\mathbf{k})+\tilde{\rho}_{\mu,\mu}^{(0)}(-\mathbf{k})\right]}{k^2+\kappa_D^2} \qquad \text{(S8)}$$

is the energy of the dielectric core of molecule ν in the electric field created by molecule μ (here $\nu\neq\mu$); $\tilde{\rho}_{\nu,\nu}^{(0)}(\mathbf{k})$ is the Fourier transform of the charge density induced on the dielectric core of molecule ν in the absence of the second molecule; and $\tilde{\rho}_{\nu,\mu}^{(1)}(\mathbf{k})$ is the first order term in the series of image charges induced on the dielectric core of molecule ν by molecule μ.

The energy of braids in non-polar media, e.g., α-helix coiled coils, may also be calculated from Eqs. (S6) -(S8) by utilizing the corresponding ε and setting $\tilde{\rho}_\nu^{ind}(\mathbf{k})=0$ as well as $\kappa_D=0$ (see Ref. (1)).

Box 1: Summation of image charges and image-charge interactions

The density of induced charges at the surface of molecule ν may be calculated with the help of the following series

$$\rho_\nu^{ind} = \sum_{n=0}^{\infty}\left[\rho_{\nu,\nu}^{(2n)} + \rho_{\nu,\mu}^{(2n+1)}\right]_{\nu\neq\mu} \tag{B1.1}$$

Here $\rho_{\nu,\nu}^{(0)} \sim \rho_\nu$ is the charge density on the dielectric core ν induced by the electric field of ρ_ν in the absence of the second molecule, $\rho_{\nu,\mu}^{(1)}$ is the charge density on the core ν induced by the electric field of $\rho_\mu + \rho_{\mu,\mu}^{(0)}$. At $m > 1$, $\rho_{\nu,\nu}^{(2n)}$ and $\rho_{\nu,\mu}^{(2n+1)}$ are the charge densities on the core ν induced by the electric field of $\rho_{\mu,\nu}^{(2n-1)}$ and $\rho_{\mu,\mu}^{(2n)}$, respectively. Since the electric field of $\rho_\mu + \rho_{\mu,\mu}^{(0)}$ propagates through electrolyte to induce $\rho_{\nu,\mu}^{(1)}$, we find that $\rho_{\nu,\mu}^{(1)} < 2\rho_\mu \exp\left(-\kappa_D d\right)$, where d is the surface-to-surface separation between the molecules. In general, $\rho_{\nu,\nu}^{(2n)} < 2\rho_\nu \exp\left(-2n\kappa_D d\right)$ and $\rho_{\nu,\mu}^{(2n+1)} < 2\rho_\mu \exp\left[-\left(2n+1\right)\kappa_D d\right]$. Due to rapid, exponential convergence of this series, the contribution from $\rho_{\nu,\mu}^{(3)}$ and higher order images into the electrostatic energy can usually be neglected. After the corresponding truncation of the series, we find

$$E_{BR}(R) \approx \left[E_{1,2}(R) + E_{2,1}(R)\right]/2 + E_{1,1}(R) + E_{2,2}(R) \tag{B1.2}$$

where

$$E_{\nu,\mu}(R)\Big|_{\nu\neq\mu} = \frac{4\pi}{\varepsilon}\int d^3\mathbf{k}\,\frac{\left[\tilde{\rho}_\nu(\mathbf{k}) + \tilde{\rho}_{\nu,\nu}^{(0)}(\mathbf{k}) + \tilde{\rho}_{\mu,\nu}^{(1)}(\mathbf{k})\right]\tilde{\rho}_\mu(-\mathbf{k})}{k^2 + \kappa_D^2} \tag{B1.3}$$

and

$$E_{\nu,\nu}(R) = \frac{2\pi}{\varepsilon}\int d^3\mathbf{k}\,\frac{\left[\tilde{\rho}_{\mu,\nu}^{(1)}(\mathbf{k}) + \tilde{\rho}_{\nu,\nu}^{(2)}(\mathbf{k})\right]\tilde{\rho}_\nu(-\mathbf{k})}{k^2 + \kappa_D^2}\,. \tag{B1.4}$$

In Eq. (B1.3), we have taken into account that the contribution into $E_{BR}(R)$ originating from $\tilde{\rho}_{\nu,\nu}^{(2)}(\mathbf{k})\tilde{\rho}_\mu(-\mathbf{k})$ is of the same order as the contribution from $\tilde{\rho}_{\mu,\nu}^{(3)}(\mathbf{k})\tilde{\rho}_\mu(-\mathbf{k})$ in Eq.(B1.4), so that both should be neglected.

Eqs. (B1.2)-(B1.4) may be further simplified by taking into account the reciprocity of electrostatic interactions, i.e., that the energy of charge j_1 in the electric field created by charge j_2 is equal to the energy of the charge j_2 in the electric field created by the charge j_1. We may then use that $E_{1,2}(R)=E_{2,1}(R)$. Furthermore, $E_{1,2}(R)$ defined by Eq. (B1.3) is equal to the energy of molecule 2 in the electric field created by the density of fixed charges ρ_1^* immersed directly in the electrolyte solution, where $\tilde{\rho}_1^*(\mathbf{k}) = \tilde{\rho}_1(\mathbf{k}) + \tilde{\rho}_{1,1}^{(0)}(\mathbf{k})$. From the reciprocity, this energy is equal to the energy of fixed charges ρ_1^* in the electric field created by the molecule 2 (in the absence of the dielectric core of molecule 1). The latter energy is given by Eq. (S7). The same reciprocity argument shows that the energy defined by Eq. (B1.4) is equal to the energy defined by Eq. (S8).

Below we derive expressions for $\tilde{\rho}_\nu(\mathbf{k})$ and $\tilde{\rho}_{\nu,\nu}^{(0)}(\mathbf{k})$ to the first order in small tilt angle α of the molecules in the braid (Section A.2) and calculate $E_{1,2}(R)$ for molecules with helical patterns of surface charges (Section A.3). An expression for $E_{\nu,\nu}(R)$ for two parallel molecules, which corresponds to the braid with $\alpha = 0$, has been published before (1,6). At least for DNA braids, we found $\partial E_{\nu,\nu}(R)/\partial\alpha$ to be negligible compared to $\partial E_{1,2}(R)/\partial\alpha$ (R. Cortini and D.J. Lee, unpublished calculations). Given the negligible contribution of $\partial E_{\nu,\nu}(R)/\partial\alpha$, here we present only the final expression for $E_{\nu,\nu}(R)$ at small α. The full derivation of this expression, which is rather cumbersome, will be reported elsewhere.

A.2 Fourier Transform of the Charge Density

A.2.1 *Coordinate frames and transformations*

To calculate $\tilde{\rho}_\nu(\mathbf{k})$ and $\tilde{\rho}_{\nu,\nu}^{(0)}(\mathbf{k})$, we utilize multiple coordinate frames (Fig. S3): (i) laboratory Cartesian frame $\mathbf{r}$; (ii) local Cartesian frame $\mathbf{r}'_{\nu,j}$ for each charge j on molecule ν; and (iii) local cylindrical frame $\left(R',z',\phi'\right)_{\nu,j}$, which corresponds to the $\mathbf{r}'_{\nu,j}$ frame. The laboratory frame has the z-axis that coincides with the braid axis. The origin and orientation of each local frame are defined so that: (a) the origin lies on the centerline of the molecule; (b) the z'-axis is tangential to the centerline; (c) the charge j lies within the z'=0 plane; (d) the x' (ϕ'=0) axis points away from the z-axis of the laboratory frame (Fig. S3).

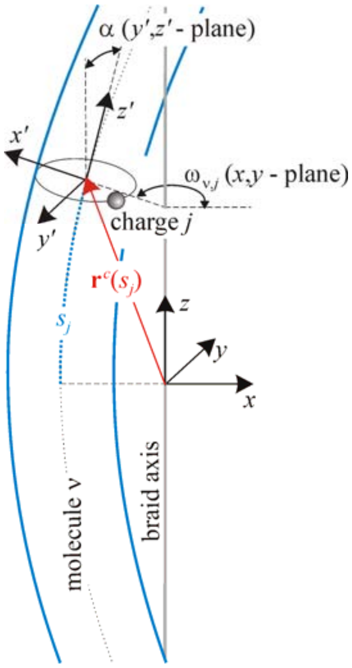

Figure S3. Schematic illustration of laboratory (*x,y,z*) and local (*x′,y′,z′*) coordinate frames.

The relationship between the $\mathbf{r}$ and $\mathbf{r}'_{\nu,j}$ coordinates is given by

$$\mathbf{r} = \mathbf{r}^c_\nu(s_j) + \vec{T}_{\nu,j}\vec{T}_\alpha \mathbf{r}'_{\nu,j}\,. \tag{S9}$$

Here s_j is the coordinate of the origin of the local coordinates along the centerline of molecule ν,

$$\mathbf{r}^c_\nu(s_j) = \begin{pmatrix} b\cos\omega_{\nu,j} \\ b\sin\omega_{\nu,j} \\ s_j\cos\alpha \end{pmatrix} \tag{S10}$$

is the coordinate of the same point in the laboratory frame and the rotations

$$\vec{T}_\alpha = \begin{pmatrix} 1 & 0 & 0 \\ 0 & \cos\alpha & -\sin\alpha \\ 0 & \sin\alpha & \cos\alpha \end{pmatrix} \tag{S11}$$

and

$$\vec{T}_{\nu,j} = \begin{pmatrix} \cos\omega_{\nu,j} & -\sin\omega_{\nu,j} & 0 \\ \sin\omega_{\nu,j} & \cos\omega_{\nu,j} & 0 \\ 0 & 0 & 1 \end{pmatrix}, \tag{S12}$$

realign the axes of the coordinates after the shift by $\mathbf{r}^c_\nu(s_j)$. In Eqs. (S10)-(S12), $b=R/2$ is the radius of the braid (distance from the braid axis to the centerline),

$$\omega_{\nu,j} = Q_c s_j + \psi_\nu\,, \tag{S13}$$

ψ_ν is the azimuthal orientation of the centerline in the laboratory frame at $s=0$ (intersection of the centerline with the $z=0$ plane of the laboratory frame), $2\pi/Q_c$ is the distance along the centerline corresponding to one full turn of the braid, and α is the tilt angle of the molecules in the braid. The relationship between Q_c and the reciprocal pitch of the braid Q as well as other important geometrical characteristics of ideal braids are discussed in Box 2.

Box 2: Braid geometry

To characterize the geometry of an ideal, straight braid formed by two molecules ν and μ, we use its reciprocal pitch Q (2π/pitch), radius b, and the tilt angle α of the molecules with respect to the braid axis (Fig. S3). We define Q as positive for right-handed and negative for left-handed braids. We define α as positive for right-handed and negative for left-handed *crossovers* between the molecules and braid axis. The sign of α is opposite to Q, since right-handed crossovers occur in left-handed braids and left-handed crossovers in right-handed braids. The value of α is related to Q as

$$Qb = -\tan\alpha\,. \tag{B2.1}$$

In our calculations, we neglect the second and higher order terms in expansion with respect to small $\sin\alpha$. We thus neglect the difference between the arc length s along the centerline of molecule ν and the corresponding length z along the braid axis, because

$$ds/dz = 1/\cos\alpha\,. \tag{B2.2}$$

Similarly, we neglect the difference between Q and Q_c (2π/centerline-arc-length per one turn of the braid), since

$$Q_c = Q\cos\alpha\,. \tag{B2.3}$$

Finally, we neglect effects associated with the centerline curvature, which is given by

$$\left|\frac{d^2\mathbf{r}^c_\nu(s)}{ds^2}\right| = \frac{(\sin\alpha)^2}{b}\,, \tag{B2.4}$$

where $\mathbf{r}^c_\nu(s)$ is the coordinate of point s on the centerline.

To calculate $\tilde{\rho}_\nu(\mathbf{k}) + \tilde{\rho}^{(0)}_{\nu,\nu}(\mathbf{k})$, we first determine the Fourier transform for each point charge and its image in $(R',z',\phi')_{\nu,j}$ coordinates associated with this charge. Then we recalculate the Fourier transforms in the laboratory frame, using the relationships between the coordinate frames discussed below. Finally, we sum the contributions of all point charges.

A.2.2 *Arbitrary patterns of surface charges*

The Fourier transform of each image contributing to $\rho^{(0)}_{\nu,\nu}$ is most conveniently determined in $(R',z',\phi')_{\nu,j}$ coordinates. Indeed, the surface density of a point charge j in these coordinates is

$$\sigma_\nu(z',\phi';j) = \frac{e_0 q_j}{a}\,\delta(z')\,\delta(\phi' - \phi'_{\nu,j})\,. \tag{S14}$$

Here a is the dielectric core radius; e_0 is the elementary charge; q_j is the charge number (valence), which may be negative or positive; $\delta(x)$ is the Dirac delta function; and $\phi'_{\nu,j}$ is the azimuthal coordinate of the charge. The cylindrical Fourier transform of $\sigma_\nu(z',\phi';j)$ is

$$\tilde{\sigma}_\nu\left(k'_z,m;j\right)=\frac{e_0 q_j}{2\pi a}e^{im\phi'_{\nu,j}}, \qquad \text{(S15)}$$

where

$$\tilde{\sigma}\left(k'_z,m\right)=\frac{1}{2\pi}\int_0^{2\pi}d\phi'\int_{-\infty}^{\infty}dz'\sigma\left(z',\phi'\right)e^{im\phi'+ik'_z z'} \qquad \text{(S16)}$$

and

$$\sigma\left(z',\phi'\right)=\frac{1}{2\pi}\sum_{m=-\infty}^{\infty}\int_{-\infty}^{\infty}dk'_z\tilde{\sigma}\left(k'_z,m\right)e^{-im\phi'-ik'_z z'}. \qquad \text{(S17)}$$

The cylindrical Fourier transform of the corresponding image charge $\sigma^{(0)}_{\nu,\nu}(z',\phi';j)$ is given by (6)

$$\tilde{\sigma}^{(0)}_{\nu,\nu}(k'_z,m;j)\approx t_m\left(k'_z\right)\tilde{\sigma}_\nu(k'_z,m;j), \qquad \text{(S18)}$$

where

$$t_m(x)=-\frac{K_m\left(a\sqrt{\kappa_D^2+x^2}\right)I'_m\left(a\sqrt{\kappa_D^2+x^2}\right)}{I_m\left(a\sqrt{\kappa_D^2+x^2}\right)K'_m\left(a\sqrt{\kappa_D^2+x^2}\right)}, \qquad \text{(S19)}$$

$K_m(x)$, $I_m(x)$, $K'_m(x)$, and $I'_m(x)$ are the modified Bessel functions of the order m and their derivatives, respectively.

Note that Eq. (S18) was derived for straight cylinders with a dielectric constant much smaller than the dielectric constant of water (6). Dielectric cores of braided DNA molecules are curved rather than straight, but this curvature is proportional to $(\sin\alpha)^2$ (Box 2).

To the first order in $\sin\alpha$, the effect of this curvature on the charge density may be neglected. The volume density $\rho_\nu\left(\mathbf{r}';j\right)$ of charge j on molecule ν in its $\mathbf{r}'_{\nu,j}$ coordinate frame is related to $\sigma_\nu(z',\phi';j)$ by

$$\rho_\nu\left(\mathbf{r}';j\right)=\delta\left(R'-a\right)\sigma_\nu(z',\phi';j). \qquad \text{(S20)}$$

The Fourier transform $\tilde{\rho}_\nu(\mathbf{k})$ in laboratory coordinates is related to Fourier transforms $\tilde{\rho}_\nu\left(\mathbf{k}';j\right)$ of $\rho_\nu\left(\mathbf{r}';j\right)$ in $\mathbf{r}'_{\nu,j}$ coordinates by

$$\tilde{\rho}_\nu(\mathbf{k})=\sum_j\exp\left[i\mathbf{k}\cdot\mathbf{r}^c_\nu(s_j)\right]\tilde{\rho}_\nu\left(\overleftrightarrow{T}_\alpha^{-1}\overleftrightarrow{T}_{\nu,j}^{-1}\mathbf{k};j\right), \qquad \text{(S21)}$$

as follows from substitution of Eq. (S9) into Eq. (S5). To the first order in $\sin\alpha$ at $|\sin\alpha| << 1$,

$$\mathbf{k}\cdot\mathbf{r}^c_\nu(s_j)\approx Kb\cos\left(\phi_{\mathbf{K}}-\omega_{\nu,j}\right)+k_z s_j, \qquad \text{(S22)}$$

where $\mathbf{k}\equiv(K,k_z,\phi_{\mathbf{K}})$ in cylindrical coordinates and we replaced $s_j\cos\alpha$ with s_j. After substitution of Eq. (S22) into Eq. (S21) and utilizing the Jacobi-Anger series

$$e^{ix\cos\phi}=\sum_{n=-\infty}^{\infty}J_n(x)e^{-in(\phi-\pi/2)}, \qquad \text{(S23)}$$

where $J_n(x)$ is the Bessel function of the order n, we find

$$\tilde{\rho}_\nu(\mathbf{k})\approx\sum_{n=-\infty}^{\infty}J_n\left(Kb\right)\sum_j e^{-in\left(\phi_{\mathbf{K}}-\omega_{\nu,j}-\pi/2\right)+ik_z s_j}\tilde{\rho}_\nu\left(\overleftrightarrow{T}_{-\alpha}\overleftrightarrow{T}_{\nu,j}^{-1}\mathbf{k};j\right) \qquad \text{(S24)}$$

To the first order in $\sin\alpha$, substitution of Eqs. (S11), (S12), (S17), and (S20) into Eq. (S5) yields

---

$$\tilde{\rho}_\nu\left(\overleftrightarrow{T}_{-\alpha}\overleftrightarrow{T}_{\nu,j}^{-1}\mathbf{k};j\right)\approx\frac{a}{(2\pi)^{3/2}}\int_0^{2\pi}d\phi'\sum_{m=-\infty}^{\infty}e^{iKa\cos\left(\phi_{\mathbf{K}}-\omega_{\nu,j}-\phi'\right)+ik_z a\sin\alpha\sin\phi'-im\phi'}\tilde{\sigma}_\nu\left(\left[k_z-K\sin\left(\phi_{\mathbf{K}}-\omega_{\nu,j}\right)\sin\alpha\right],m;j\right). \qquad \text{(S25)}$$

After two additional applications of the Jacobi-Anger series, Eqs. (S24), (S25) may be reduced to

$$\begin{aligned}\tilde{\rho}_\nu(\mathbf{k})\approx{}&\frac{a}{(2\pi)^{1/2}}\sum_{n,n',n''=-\infty}^{\infty}J_n\left(Kb\right)J_{n'}\left(Ka\right)J_{n''}\left(k_z a\sin\alpha\right)\\&\times\sum_j\tilde{\sigma}_\nu\left(\left[k_z-K\sin\left(\phi_{\mathbf{K}}-\omega_{\nu,j,l}\right)\sin\alpha\right],n''+n';j\right)\quad.\\&\times e^{i(n+n')\left(\omega_{\nu,j}-\phi_{\mathbf{K}}+\pi/2\right)+ik_z s_j}\end{aligned} \qquad \text{(S26)}$$

The relationship between $\tilde{\rho}^{(0)}_{\nu,\nu}(\mathbf{k})$ and $\tilde{\sigma}^{(0)}_{\nu,\nu}(k'_z,m;j)$ is exactly the same. Then, the substitution of Eqs. (S13) (S15), (S18) into Eq. (S26) leads to

$$\begin{aligned}&\tilde{\rho}_\nu(\mathbf{k})+\tilde{\rho}^{(0)}_{\nu,\nu}(\mathbf{k})\\&\quad\approx\frac{e_0}{(2\pi)^{3/2}}\sum_{n,n',n''=-\infty}^{\infty}J_n\left(Kb\right)J_{n'}\left(Ka\right)J_{n''}\left(k_z a\sin\alpha\right)\\&\quad\times\sum_j\left(1+t_{n''+n'}\left[k_z-K\sin\left(\phi_{\mathbf{K}}-Qs_j-\psi_\nu\right)\sin\alpha\right]\right),\\&\qquad\times q_j e^{i(n+n')\left(Qs_j+\psi_\nu-\phi_{\mathbf{K}}+\pi/2\right)+i(n'+n'')\phi'_{\nu,j}+ik_z s_j}\end{aligned} \qquad \text{(S27)}$$

where we used that $Q_c\approx Q$, to the first order in $\sin\alpha$ (Box 2). Eq. (S27) defines $\tilde{\rho}_\nu(\mathbf{k})+\tilde{\rho}^{(0)}_{\nu,\nu}(\mathbf{k})$ for an arbitrary pattern of discrete charges on the surface of the

Box 3: Crick's formula for ideal helical chains

Consider the simplest example of ideal helical chains formed by equally spaced charges with $q_j=1$ and $s_j=l_c j$, where l_c is the spacing between the charges along the centerline. When braiding of such chains does not introduce extra twist deformation within each chain, e.g., when the chains have free ends and can relax the twist, we find

$$\phi'_{\nu,j} = g_\nu l_c j + \phi_\nu - \omega_{\nu,j} \tag{B3.1}$$

Here ϕ_ν is the phase of the charges within chain ν and g_ν is the reciprocal helical pitch of the chain. The subtraction of $\omega_{\nu,j}$ accounts for the rotation of the local coordinate system, preserving the intrinsic twist of the chain.

For such chains, substitution of $q_j=1$, $s_j=l_c j$, Eq. (S13), and Eq. (B3.1) into Eq. (S26) yields

$$\tilde{\rho}_\nu(\mathbf{k}) = \frac{e_0}{(2\pi)^{3/2}} \sum_{n,n',n''=-\infty}^{\infty} J_n(Kb) J_{n'}(Ka) J_{n''}(k_z a\sin\alpha) e^{i(n+n')(\pi/2-\phi_{\mathbf{K}})+i(n-n'')\psi_\nu} \sum_j e^{i\left[k_z+(n-n'')Q+(n''+n')g_\nu\right]l_c j} . \tag{B3.2}$$

For chains containing a large number of charges N_ν, this equations reduces to

$$\tilde{\rho}_\nu(\mathbf{k}) = \frac{N_\nu e_0}{(2\pi)^{3/2}} \sum_{n,n',n''=-\infty}^{\infty} J_n(Kb) J_{n'}(Ka) J_{n''}(k_z a\sin\alpha) e^{i(n+n')(\pi/2-\phi_{\mathbf{K}})+i(n-n'')\psi_\nu} \sum_{J=-\infty}^{\infty} \delta_{-k_z,(n-n'')Q+(n''+n')g-2\pi J/l_c} . \tag{B3.3}$$

Here we used that, for equally spaced charges, the sum over j yields N_ν for any k_z satisfying the following selection rule

$$\left[k_z + (n-n'')Q + (n''+n')g_\nu\right]l_c = 2\pi J , \tag{B3.4}$$

where J is an arbitrary integer.

An analogue of Eq. (B3.3) for the Fourier transform of the density of atoms in supercoiled ideal helical chains, which may be obtained by replacing e_0 with 1, was originally derived by F. Crick (5). It played an important role, e.g., for understanding x-ray diffraction from coiled coils of α-helices.

dielectric core of molecule ν, to the first order in $\sin\alpha$. For sufficiently long molecules, the sum over j can be calculated, simplifying Eq. (S27) and enabling us to calculate the other sums and integrals in Eq. (S7). The simplest example of ideal helical chains of equally spaced charges is discussed in Box 3.

A.2.3 *Ideal, DNA-like double helices*

For DNA, we calculate the Fourier transforms of the charge density separately for phosphate groups and bound counterions. We begin from an approximation in which we assume that phosphate groups form an ideal helical pattern with the reciprocal pitch g. Then, phosphate group locations may be described with

$$\phi'_{\nu,2l-1} = g s_{2l} + \Phi_\nu - \tilde{\phi}_s - \omega_{\nu,2l} \tag{S28}$$

$$\phi'_{\nu,2l} = g s_{2l} + \Phi_\nu + \tilde{\phi}_s - \omega_{\nu,2l} \tag{S29}$$

$$s_{2l-1} = s_{2l} \tag{S30}$$

Here the index l labels DNA base pairs, $j=2l-1$ and $j=2l$ are two phosphate groups within the same base pair l, Φ_ν is the orientation of the center of the minor groove at $s=0$), $\tilde{\phi}_s \approx 0.4\pi$ is the azimuthal half-width of the minor groove. The subtraction of $\omega_{\nu,j}$ accounts for the rotation of the local $(R', z', \phi')_{\nu,j}$ coordinate frame, so that the molecule retains its intrinsic twist g in the braid (rotation angle of phosphate chains around the centerline per unit length of the centerline).

Setting $q_j = -1$, substituting Eqs. (S13), (S28)-(S30) into Eq. (S27), and using that $Q_c \approx Q$ (Box 2) we find

$$\begin{aligned}
&\tilde{\rho}_\nu(\mathbf{k}) + \tilde{\rho}^{(0)}_{\nu,\nu}(\mathbf{k}) \\
&\quad\approx \frac{e_0}{(2\pi)^{3/2}} \sum_{n,n',n''=-\infty}^{\infty} J_n(Kb) J_{n'}(Ka) J_{n''}(k_z a\sin\alpha)\, \zeta_{n'+n''} \\
&\quad\times e^{i(n+n')(\pi/2-\phi_{\mathbf{K}})+i(n-n'')\psi_\nu+i(n'+n'')\Phi_\nu} \sum_j e^{i\left(k_z+(n-n'')Q+(n'+n'')g\right)s_j} \\
&\quad\times\left[1 + t_{n'+n''}\left(k_z - K\sin\alpha\sin\left(\phi_{\mathbf{K}} - Q s_l - \psi_\nu\right)\right)\right]
\end{aligned} , \tag{S31}$$

where $\zeta_m = -\cos\left(m\tilde{\phi}_s\right)$.

To the first order in $\sin\alpha$, Eq. (S31) may then be rewritten as

$$\begin{aligned}
&\tilde{\rho}_\nu(\mathbf{k}) + \tilde{\rho}^{(0)}_{\nu,\nu}(\mathbf{k}) \\
&\quad\approx \frac{2Le_0}{\bar{h}(2\pi)^{3/2}} \sum_{n,n',n''=-\infty}^{\infty} J_n(Kb) J_{n'}(Ka) J_{n''}(k_z a\sin\alpha) \\
&\quad\times\left[1 + t_{n'+n''}(k_z) - K\sin\alpha\sin\left(\phi_{\mathbf{K}} - \psi_\nu\right) t'_{n'+n''}(k_z)\right]\zeta_{n'+n''} \\
&\quad\times e^{i(n+n')(\pi/2-\phi_{\mathbf{K}})+i(n-n'')\psi_\nu+i(n'+n'')\Phi_\nu}\, \delta_{-k_z,(n-n'')Q+(n'+n'')g}
\end{aligned} , \tag{S32}$$

where $t'_m(k_z) \equiv \partial t_m(k_z)/\partial k_z$. Here, we have taken into account that for molecules with the length $L >> 2\pi/Q$,

$$\sum_j e^{ixs_j} \approx \frac{2L}{\bar{h}} \delta_{x,0}\,, \tag{S33}$$

where $\bar{h}$ is the average axial rise per base pair and $\delta_{x,y}$ is the Kroenecker delta ($\delta_{x,y} = 1$ at $x = y$ and $\delta_{x,y} = 0$ at $x \neq y$). For ideal helical chains with equally spaced charges, one must also account for $xs_j = 2\pi J$ with nonzero integer values of J (Box 3). For DNA, however, the Fourier modes with $J \neq 0$ are suppressed by sequence-related and thermal fluctuations in the twist and rise between adjacent base pairs (see (1) and Box 4).

Note that the specific locations of phosphate charges within the double helix are determined entirely by the coefficient $\zeta_m = -\cos\left(m\tilde{\phi}_s\right)$. All other factors in Eq. (S32) simply reflect the general helical symmetry of DNA and the braid.

For bound counterions, we cannot assume fixed locations on DNA surface. Instead, we suppose that these charges are mobile and their density is determined primarily by the molecule to which they are bound. In this case, we may expect the average surface charge density of bound counterions to follow the helical symmetry of the molecule.

Within these assumptions, the total (phosphate and counterion) charge density $\tilde{\rho}_\nu(\mathbf{k}) + \tilde{\rho}^{(0)}_{\nu,\nu}(\mathbf{k})$ in DNA braids is described by Eq. (S32) as well. However, for the total charge density

$$\zeta_m = \zeta_m^+ - \cos\left(m\tilde{\phi}_s\right), \tag{S34}$$

where ζ_m^+ determines the counterion contribution.

Similar to our previous studies of interactions between straight DNA molecules (1), we utilize a phenomenological model for ζ_m^+, which distinguishes three types of counterion binding sites: (i) random, (ii) in the middle of the minor groove, and (iii) in the middle of the major groove. Within this model (1)

$$\zeta_m = \left[f_1 + f_2 (-1)^m + (1 - f_1 - f_2)\delta_{m,0} \right]\theta - \cos\left(m\tilde{\phi}_s\right), \tag{S35}$$

where f_1, f_2, and (1-f_1-f_2) are the fractions of ions bound in the minor groove, major groove and randomly, and θ is the total fraction of negative charge compensated by bound counterions.

A.3. Interaction Energy

A.3.1 *Direct interactions*

Substitution of Eq. (S32) into Eq. (S7) yields

$$\frac{E_{1,2}(R)}{k_B T} \approx L\left(\Upsilon_1 + \Upsilon_2 + \Upsilon_3\right). \tag{S36}$$

where to the first order in $\sin\alpha$

$$\Upsilon_1 = \frac{l_B}{\pi l_c^2} \int_{-\infty}^{\infty} dk_z \int_0^{\infty} K dK \int_0^{2\pi} d\phi_{\mathbf{K}} \sum_{n,n',m,m'=-\infty}^{\infty} (-1)^{m+m'} \left[\frac{J_n(Kb) J_{n'}(Ka) J_m(Kb) J_{m'}(Ka)}{K^2 + k_z^2 + \kappa_D^2} \right] , \tag{S37}$$
$$\times \left[1 + t_{n'}(k_z)\right]\left[1 + t_{m'}(-k_z)\right] \zeta_{n'} \zeta_{m'} e^{i(n+n'+m+m')(\pi/2 - \phi_{\mathbf{K}}) + in'\Phi_1 + in\psi_1 + im'\Phi_2 + im\psi_2} \delta_{(n'+m')g,-(n+m)Q}\, \delta\left(k_z + nQ + n'g\right)$$

$$\Upsilon_2 = \frac{l_B a \sin\alpha}{2\pi l_c^2} \int_{-\infty}^{\infty} k_z dk_z \int_0^{\infty} K dK \int_0^{2\pi} d\phi_{\mathbf{K}} \sum_{n,n',n'',m,m',m''=-\infty}^{\infty} (-1)^{m+m'} \left[\frac{J_n(Kb) J_{n'}(Ka) J_m(Kb) J_{m'}(Ka)}{K^2 + k_z^2 + \kappa_D^2} \right]$$
$$\times \left[1 + t_{n'+n''}(k_z)\right]\left[1 + t_{m'+m''}(-k_z)\right] \zeta_{n'+n''} \zeta_{m'+m''} e^{i(n+n'+m+m')(\pi/2 - \phi_{\mathbf{K}}) + i(n'+n'')\Phi_1 + i(n-n'')\psi_1 + i(m'+m'')\Phi_2 + i(m-m'')\psi_2} , \tag{S38}$$
$$\times \left[\delta_{m'',0}\left(\delta_{n'',1} - \delta_{n'',-1}\right) - \delta_{n'',0}\left(\delta_{m'',1} - \delta_{m'',-1}\right) \right] \delta_{(n''-n+m''-m)Q,(n'+n''+m'+m'')g}\, \delta\left(k_z + n'g + n''g\right)$$

$$\Upsilon_3 = \frac{l_B \sin\alpha}{\pi l_c^2} \int_{-\infty}^{\infty} dk_z \int_0^{\infty} K^2 dK \int_0^{2\pi} d\phi_{\mathbf{K}} \sum_{n,n',m,m'=-\infty}^{\infty} (-1)^{m+m'} \left[\frac{J_n(Kb) J_{n'}(Ka) J_m(Kb) J_{m'}(Ka)}{K^2 + k_z^2 + \kappa_D^2} \right] \delta_{(n'+m')g,-(n+m)Q}\, \delta\left(k_z + n'g\right) .$$
$$\times \left\{ t'_{m'}(-k_z)\left[1 + t_{n'}(k_z)\right] \sin\left(\phi_{\mathbf{K}} - \psi_2\right) - t'_{n'}(k_z)\left[1 + t_{m'}(-k_z)\right] \sin\left(\phi_{\mathbf{K}} - \psi_1\right) \right\} \zeta_{n'} \zeta_{m'} e^{i(n+n'+m+m')(\pi/2 - \phi_{\mathbf{K}}) + in'\Phi_1 + in\psi_1 + im'\Phi_2 + im\psi_2} \tag{S39}$$

Here $l_B = e_0^2 / (\varepsilon k_B T)$ is the Bjerum length (≈ 7 Å in water) and l_c is the length along the DNA centerline per one phosphate charge (≈ 1.7 Å). To obtain Eqs. (S37)-(S39), we used that to the first order in $\sin\alpha$

$$J_m(k_z a \sin\alpha) \approx \delta_{m,0} + \frac{k_z a \sin\alpha}{2}\left(\delta_{m,1} - \delta_{m,-1}\right) \tag{S40}$$

and

$$Q \approx -\sin\alpha / b \tag{S41}$$

(see Box 2) as well as that

$$\frac{L}{2\pi}\delta_{-k_z,(n-n'')Q+(n'+n'')g} \approx \delta\left(k_z+\left[n-n''\right]Q+\left[n'+n''\right]g\right) \tag{S42}$$

at $L/2\pi >> Q^{-1}, g^{-1}$.

To calculate the integrals in Eqs. (S37)-(S39), we utilize that

$$\int_0^{2\pi} e^{-i(n+n'+m'+m'')\phi_{\mathbf{K}}}\, d\phi_{\mathbf{K}} = 2\pi\delta_{n+n'+m'+m'',0} \, . \tag{S43}$$

After eliminating most of the sums with the help of the delta indices, we take into account that

$$\sum_{m=-\infty}^{\infty} J_m(Kb)J_{N-m}(Kb) = J_N(2Kb) \equiv J_N(KR), \tag{S44}$$

as well as that ((7), Eq. 8.11.51)

$$\int_0^{\infty} KdK \frac{J_{n-m}(KR)J_n(Ka)J_m(Ka)}{K^2+\kappa^2} \qquad (R>2a)$$
$$= (-1)^m K_{n-m}(\kappa R)I_n(\kappa a)I_m(\kappa a) \tag{S45}$$

and

$$\left[1-t_n(ng)\right]^2\left[I_n(\kappa_n a)\right]^2 = \frac{1}{(\kappa_n a)^2\left[K_n'(\kappa_n a)\right]^2}, \tag{S46}$$

where

$$\kappa_n = \sqrt{\kappa_D^2+n^2g^2} \, . \tag{S47}$$

After straightforward algebra, we find

$$\frac{E_{1,2}(R)}{k_BT} \approx L\sum_{n=-\infty}^{\infty}(-1)^n u_n \cos\left[n\left(\Phi_1-\Phi_2\right)\right] \tag{S48}$$

where

$$u_n \approx \frac{2l_B}{l_c^2}\frac{\zeta_n^2\left[K_0(\kappa_n R)+2ga\sin\alpha\dfrac{n^2K_1(\kappa_n R)}{\kappa_n a}\right]}{(\kappa_n a)^2\left[K_n'(\kappa_n a)\right]^2}. \tag{S49}$$

Note that at α=0 we recover the expression reported before for parallel, straight helices (1, 6). The series rapidly converges and, under most conditions, only the terms with $|n| \le 3$ are relevant.

A.3.1 *Image-charge interactions*

A calculation of $E_{1,1}(R)$ and $E_{2,2}(R)$ yields (R. Cortini and D.J. Lee, unpublished)

$$\frac{E_{1,1}(R)+E_{2,2}(R)}{k_BT} \approx L\sum_{n=-\infty}^{\infty}u_n^{im}, \tag{S50}$$

where

$$u_n^{im} \approx \frac{2l_B}{l_c^2}\frac{\zeta_n^2\,\Omega_{n,n}(\kappa_n R,\kappa_n a)}{(\kappa_n a)^2\left[K_n'(\kappa_n a)\right]^2} + ag\sin\alpha\frac{4l_B}{l_c^2}\frac{n\zeta_n^2\tilde{\Omega}_{n,n}(\kappa_n R,\kappa_n a)}{(\kappa_n a)^2\left[K_n'(\kappa_n a)\right]^2}, \tag{S51}$$

$$\Omega_{n,n}(x,y) = -\sum_{j=-\infty}^{\infty}\left[K_{n-j}(x)\right]^2\frac{I_j'(y)}{K_j'(y)} \tag{S52}$$

$$\tilde{\Omega}_{n,n}(x,y) = \sum_{j=-\infty}^{\infty}\frac{K_{n+j+1}(x)K_{n+j}(x)}{y\left[K_j'(y)\right]^2} \times\left[1+2jI_j'(y)K_j'(y)+\frac{j^2}{y^2}\right] \tag{S53}$$

The first term in Eq. (S51), which describes image-charge interactions between straight, parallel helices, was described previously (1, 6). The second term in Eq. (S51) provides a negligible contribution to $E_{BR}(R)$ and may be omitted for the purpose of the present study. Its derivation, which is more complicated than for the corresponding term in Eq. (S49), will be reported elsewhere.

B. FREE ENERGY OF DNA BRAIDS

B.1 Nonideal Double Helices

Our first step in evaluating the free energy of DNA braids is to account for sequence-related and thermal distortions of the double helix, since the structure of real DNA is neither ideal nor rigid. These distortions may involve twisting, stretching, and undulations. We base their analysis on lessons from previous studies of parallel pairs and columnar assemblies of DNA (1-3, 8). These studies revealed that torsional (twisting) and stretching distortions of the double helix are always important since they affect the alignment of charged helical strands on opposing surfaces. Undulations do not have a significant effect on this alignment and contribute to the free energy only at larger interaxial distances. At distances expected in DNA braids (Fig. 3 of the main text), undulations are suppressed by electrostatic interactions and their contribution to the free energy is small (2). In braids, undulations are further suppressed by winding of the molecules around each other. Given the expectation of only a small contribution of undulations to the free energy and the complexity of their calculation within braid geometry, here we simply neglect this contribution. In other words, we assume that DNA centerlines form an ideal, symmetric braid.

To account for torsional and stretching distortions of DNA within such braids, we utilize the same approach as in previous studies of interactions between parallel molecules (1-3, 8). Based on the arguments summarized in Box 4, we approximate the electrostatic interaction energy within a braid composed of nonideal double helices as

$$\frac{E_{BR}}{k_BT} \approx \int_0^L ds\sum_{n=-\infty}^{\infty}\left[(-1)^n\cos\left[n\Delta\Phi(s)\right]u_n+u_n^{im}\right]. \tag{S54}$$

This expression is similar to Eqs. (S6), (S48)-(S53), except here $\Delta\Phi(s)=\Phi_1(s) - \Phi_2(s)$, where

Box 4: Interaction between nonideal double helices

To account for twisting and stretching distortions of the double helix, we describe the locations of phosphate groups with

$$\phi'_{\nu,2l-1} = \bar{g}s_{2l} + \Phi_{\nu,2l} - \tilde{\phi}_s - \omega_{\nu,2l}\,, \quad \phi'_{\nu,2l} = \bar{g}s_{2l} + \Phi_{\nu,2l} + \tilde{\phi}_s - \omega_{\nu,2l} \qquad \text{(B4.1)}$$

Similar to Eqs. (S28)-(S30), $s_{2l} = s_{2l\text{-}1}$ is the centerline coordinate of base pair l, but $\Phi_{\nu,2l} \equiv \Phi_\nu(s_{2l})$ is now the helical phase of base pair l, which is defined by Eq. (S55) and depends on l. Instead of Eqs. (S36)-(S39), we then find

$$\begin{aligned}\frac{E_{1,2}(R)}{k_B T} \approx & \int_{-\infty}^{\infty} dk_z \int_0^{\infty} K dK \int_0^{2\pi} d\phi_{\mathbf{K}} \sum_{n,n',n'',m,m',m''} \mathcal{G}_{n,n',n'',m,m',m''}\left(k_z, K, \phi_{\mathbf{K}}\right) \\ & \times \sum_l e^{i\left[\left(n+m-n''-m''\right)Q + \left(n'+m'+n''+m''\right)\bar{g}\right]s_{2l} + i\left(n'+n''\right)\Phi_{1,2l} + i\left(m'+m''\right)\Phi_{2,2l}} \sum_{l'} e^{i\left(-k_z + \left(m-m''\right)Q + \left(m'+m''\right)\bar{g}\right)\left(s_{2l'}-s_{2l}\right) + i\left(m'+m''\right)\left(\Phi_{2,2l'}-\Phi_{2,2l}\right)}\,,\end{aligned} \qquad \text{(B4.2)}$$

where the summation is performed over base pairs and

$$\begin{aligned}\mathcal{G}_{n,n',n'',m,m',m''}\left(k_z, K, \phi_{\mathbf{K}}\right) = & \frac{8 l_B}{(2\pi)^2} (-1)^{m+m'} \frac{J_n(Kb) J_m(Kb) J_{n'}(Ka) J_{m'}(Ka) J_{n''}(k_z a \sin\alpha) J_{m''}(-k_z a \sin\alpha)}{K^2 + k_z^2 + \kappa_D^2} \\ & \times \left[1 + t_{n'+n''}(k_z) - K \sin\alpha \sin\left(\phi_{\mathbf{K}} - \psi_1\right) t'_{n'+n''}(k_z)\right]\left[1 + t_{m'+m''}(-k_z) + K \sin\alpha \sin\left(\phi_{\mathbf{K}} - \psi_2\right) t'_{m'+m''}(-k_z)\right] \\ & \times \zeta_{n'+n''} \zeta_{m'+m''} e^{i(n+n'+m+m')(\pi/2 - \phi_{\mathbf{K}}) + i(n-n'')\psi_1 + i(m-m'')\psi_2}\,.\end{aligned} \qquad \text{(B4.3)}$$

We may now take into account that the variation of $\Phi_{\nu,l}$ with l is relatively slow. For individual DNA molecules,

$$\left\langle \left[\Phi_{\nu,2l} - \Phi_{\nu,2l'}\right]^2 \right\rangle = \frac{|l-l'|}{\lambda_c / \bar{h}}\,, \qquad \text{(B4.4)}$$

where λ_c is the helical coherence length of DNA; intermolecular interactions only reduce $<[\Phi_{\nu,2l} - \Phi_{\nu,2l'}]^2>$ (2-4). Since $\lambda_c / \bar{h} \sim 30$, $\lambda_c \kappa_D >> 1$ and only $|n' + n''| \leq 3$ are important for intermolecular interactions in the braid (section A.3), the sums over l and l' in Eq. (B4.2), contribute significantly to the energy only at

$$\left(n' + m' + n'' + m''\right)\bar{g} \approx \left(n'' + m'' - n - m\right)Q \quad \text{and} \quad k_z \approx \left(m - m''\right)Q + \left(m' + m''\right)\bar{g}\,. \qquad \text{(B4.5)}$$

After substituting Eq. (B4.5) into Eq. (B4.2) and replacing the sums over l and l' with integrals, we find

$$\begin{aligned}\frac{E_{1,2}(R)}{k_B T} \approx & \int_0^{\infty} K dK \int_0^{2\pi} d\phi_{\mathbf{K}} \sum_{n,n',n'',m,m',m''} \mathcal{G}_{n,n',n'',m,m',m''}\left[\left(m-m''\right)Q + \left(m'+m''\right)\bar{g}, K, \phi_{\mathbf{K}}\right] \delta_{\left(n'+m'+n''+m''\right)\bar{g},\left(n''+m''-n-m\right)Q} \\ & \times \left[\int_0^L \frac{ds}{\bar{h}} e^{i\left(n'+n''\right)\Phi_1(s) + i\left(m'+m''\right)\Phi_2(s)}\right] e^{-i\left(m'+m''\right)\Phi_2(s)} \int_{-\infty}^{\infty} dq_z e^{iq_z s} \int_0^L \frac{ds'}{\bar{h}} e^{-iq_z s' + i\left(m'+m''\right)\Phi_2(s')}\,,\end{aligned} \qquad \text{(B4.6)}$$

where $q_z = k_z - \left(m - m''\right)Q + \left(m' + m''\right)\bar{g}$. Taking into account that

$$\int_{-\infty}^{\infty} dq_z e^{iq_z s} \int_0^L ds' e^{-iq_z s'} \left[e^{i\left(m'+m''\right)\Phi_2(s')}\right] = 2\pi e^{i\left(m'+m''\right)\Phi_2(s)} \qquad \text{(B4.7)}$$

and calculating the remaining sums and integrals in Eq. (B4.6) as described in section A.3, we arrive at Eq. (S54).

$$\begin{aligned}\Phi_\nu(s_{2l}) &= \Phi_\nu(s_0) + \sum_{m=0}^{l}\left[\Omega_\nu\left(s_{2m}\right) - \bar{g}h_\nu(s_{2m})\right] \\ &\approx \Phi_\nu(0) + \int_0^s d\tau \frac{\Omega_\nu(\tau) - \bar{g}h_\nu(\tau)}{\bar{h}}\end{aligned} \qquad \text{(S55)}$$

is the helical phase of molecule ν at base pair l, $\Phi_\nu(0)$ is the azimuthal orientation of the center of the minor groove of molecule ν at s=0, $\Omega_\nu(s_{2m})$ and $h_\nu(s_{2m})$ are the twist and rise per base pair along the centerline (between base pairs m and m - 1). Similar to Eqs. (S6), (S48)-(S53), $\Delta\Phi(s)$ is equal to the difference between azimuthal orientations of the centers of the minor grooves of the two molecules at any s. In addition, in Eq. (S54) compared to Eqs. (S6), (S48)-(S53), the average reciprocal pitch of DNA $\bar{g}$ replaces g, and integration of the energy per unit length over the length of the molecules replaces multiplication of the same energy by L (c.f., Eq. (S48)). Both torsional and stretching deformations affect the value of $\Delta\Phi(s)$.

B.2 Energy Functional

We describe the elastic energy E_{ER} associated with these deformations as well as with bending of DNA necessary to form the braid within the elastic rod model, which is defined by Eq. (1) of the main text. After substitution of Eq. (S55) and Eq. (B2.4) into Eq. (1), we find

$$\begin{aligned}\frac{E_{ER}}{k_BT} &= 4l_p^bL\frac{\left(\sin\alpha\right)^4}{R^2}+\frac{l_p^h}{2}\sum_{\nu=1}^{2}\int_0^L ds\left[\Delta\varpi_\nu\left(s\right)\right]^2\\ &+\frac{l_p^h}{2}\sum_{\nu=1}^{2}\int_0^L ds\left[\frac{d\Phi_\nu(s)}{ds}-\frac{\Omega_\nu^0(s)-\bar{g}h_\nu^0(s)}{\bar{h}}\right]^2\end{aligned} \tag{S56}$$

where l_p^b is the bending persistence length of DNA ($l_p^b = B/k_BT$, B is the bending modulus),

$$l_p^h = \frac{C_tC_s/k_BT}{C_s+\bar{g}^2C_t} \tag{S57}$$

is the helical persistence length of DNA (C_s and C_t are the stretching and torsional elasticity moduli of DNA, respectively),

$$\begin{aligned}\Delta\varpi_\nu\left(s\right) &= \left(\frac{\bar{g}^2C_t}{C_s}\right)^{\frac{1}{2}}\frac{\Omega_\nu(s)-\Omega_\nu^0(s)}{\bar{h}}\\ &+\bar{g}\left(\frac{C_s}{\bar{g}^2C_t}\right)^{\frac{1}{2}}\frac{h_\nu(s)-h_\nu^0(\tau)}{\bar{h}}\end{aligned} \tag{S58}$$

is an independent twist-stretch deformation, which does not affect the helical phase, $\Omega_\nu^0(s)$ is the intrinsic twist, and $h_\nu^0(s)$ is the intrinsic rise per base pair along the centerline. After introducing $\Delta\Omega^0(s)=\Omega_1^0(s)-\Omega_2^0(s)$, $\Delta h^0(s)=h_1^0(s)-h_2^0(s)$, and combining Eq. (S56) with Eq. (S54), we may represent the total energy of the braid in the following form

$$\begin{aligned}\frac{E_{DNA}\left(R,\alpha\right)}{k_BT} &\approx \frac{E_0}{k_BT}+4l_p^bL\frac{\left(\sin\alpha\right)^4}{R^2}\\ &+\frac{l_p^h}{4}\int_0^L ds\left(\frac{d\Delta\Phi(s)}{ds}-\frac{\Delta\Omega^0(s)-\bar{g}\Delta h^0(s)}{\bar{h}}\right)^2,\\ &+\int_0^L ds\sum_{n=-\infty}^{\infty}\left[(-1)^n\cos\left[n\Delta\Phi\left(s\right)\right]u_n+u_n^{im}\right]\end{aligned} \tag{S59}$$

where E_0 combines all components of the energy independent of R and $\Delta\Phi(s)$. These energies are not affected by DNA braiding and therefore they do not contribute to the free energy of braid formation.

Note that in Eq. (S59) we account for the bending energy proportional to $(\sin\alpha)^4$ while we neglect electrostatic energies proportional to $(\sin\alpha)^2$. The reason behind this approximation is the large bending persistence length of DNA, which may make the bending energy comparable to the first order terms in the expansion of the electrostatic energy with respect to $\sin\alpha$ at relevant α. For additional discussion of this approximation, see the main text.

B.3 Variational Approximation

We calculate the free energy of braid formation as described in the Supplementary Material of (2). Briefly, we separate different contributions to fluctuations in the helical phase,

$$\Delta\Phi(s)=\Delta\Phi^{(0)}(s)+\delta\Phi(s)\,, \tag{S60}$$

where the first term describes static (e.g., sequence-related) distortions in the double helix structure and the second term describes thermal fluctuations. We introduce an effective energy cost of $\delta\Phi(s)$

$$\tilde{E}_{eff}=\frac{k_BT}{2}\int_0^L ds\left[\frac{l_p^h}{2}\left(\frac{d\delta\Phi(s)}{ds}\right)^2+\beta\left[\delta\Phi(s)\right]^2\right], \tag{S61}$$

where β is a variational parameter, and approximate the free energy of braid formation as

$$\begin{aligned}F_{DNA} &\approx -k_BT\ln\left[\int\exp\left(\frac{-\tilde{E}_{eff}}{k_BT}\right)\mathcal{D}\left(\delta\Phi\right)\right].\\ &+\left\langle\left\langle E_{DNA}-E_0-\tilde{E}_{eff}\right\rangle\right\rangle\end{aligned} \tag{S62}$$

Here $\mathcal{D}\left(\delta\Phi\right)$ indicates path integral over all possible "trajectories" of $\delta\Phi(s)$ and double brackets indicate averaging over thermal fluctuations with the weight factor $\exp\left(-\tilde{E}_{eff}/k_BT\right)$ plus averaging over possible realizations of $\Omega_\nu^0(s)-\bar{g}h_\nu^0(s)$.

To account for DNA flexibility we optimize the free energy of braid formation not only with respect to β but also with respect to $\Delta\Phi^{(0)}(s)$. Specifically, we look for $\Delta\Phi^{(0)}(s)$ among the following trial functions (3)

$$\begin{aligned}\Delta\Phi^{(0)}(s) &= \overline{\Delta\Phi}\\ &+\frac{1}{2\bar{h}}\int_0^L ds'\left[\Delta\Omega^0\left(s'\right)-\bar{g}\Delta h^0\left(s'\right)\right]\frac{s-s'}{\left|s-s'\right|}e^{-\left|s-s'\right|/\lambda_h}\end{aligned} \tag{S63}$$

where $\overline{\Delta\Phi}$ is the average difference between the helical phases of the two molecules within the braid and λ_h is a second variational parameter of the theory.

After minimizing with respect to both λ_h and β, as described in Supplementary Material of (2), we arrive at

$$\begin{aligned}\frac{F_{DNA}}{k_BT} &\approx 4l_p^bL\frac{(\sin\alpha)^4}{R^2}+L\frac{\left(l_p^h+\lambda\right)^2}{16\lambda_h^\star\lambda l_p^h}\\ &+L\sum_{n=-\infty}^{\infty}\left[(-1)^n\cos\left(n\overline{\Delta\Phi}\right)\exp\left(-\frac{n^2\lambda_h^\star}{2\lambda}\right)u_n+u_n^{im}\right]\end{aligned} \tag{S64}$$

where the structural adaptation length, $\lambda_h^\star$ and the difference in the average helical phases of the molecules, $\overline{\Delta\Phi}$ should be found from

$$\partial F_{DNA}/\partial\lambda_h^\star=\partial F_{DNA}/\partial\overline{\Delta\Phi}=0\,. \tag{S65}$$

The value of λ depends on the relationship between the sequences of the two molecules in the braid. When the molecules have homologous sequences,

$$\Delta\Omega^0(s) \approx 0 \text{ and } \Delta h^0(s) \approx 0 \tag{S66}$$

and

$$\lambda = l_p^h . \tag{S67}$$

When the two molecules have unrelated (and therefore uncorrelated) sequences,

$$\left\langle \left(\int_{s'}^{s} \frac{d\tau}{\bar{h}} \left[\Delta\Omega^0(\tau) - \bar{g}\Delta h^0(\tau) \right] \right)^2 \right\rangle \approx 2\frac{|s-s'|}{\lambda_c^{(0)}} \tag{S68}$$

and

$$\lambda = \lambda_c = \frac{l_p^h \lambda_c^{(0)}}{l_p^h + \lambda_c^{(0)}} , \tag{S69}$$

where λ_c (≈ 105 Å (4, 9)) is the helical coherence of DNA and $\lambda_c^{(0)}$ (≈ 150 Å (9)) is its intrinsic component (1, 2, 9).

Equations (S64)-(S69) are utilized in the main text of the paper for analysis of DNA braiding under different conditions.

References

1. Kornyshev, A. A., D. J. Lee, S. Leikin, and A. Wynveen. 2007. Structure and interactions of biological helices. Rev. Mod. Phys. 79:943-996.
2. Lee, D. J., A. Wynveen, A. A. Kornyshev, and S. Leikin. 2010. Undulations enhance the effect of helical structure on DNA interactions. J Phys Chem B 114:11668-11680.
3. Cherstvy, A. G., A. A. Kornyshev, and S. Leikin. 2004. Torsional Deformation of Double Helix in Interaction and Aggregation of DNA. J Phys Chem B 108:6508-6518.
4. Kornyshev, A. A., D. J. Lee, A. Wynveen, and S. Leikin. 2011. Signatures of DNA flexibility, interactions and sequence-related structural variations in classical X-ray diffraction patterns. Nucleic Acids Res:doi:10.1093/nar/gkr1260.
5. Crick, F. H. C. 1953. The Fourier Transform of a Coiled-Coil. Acta Crystallographica 6:685-689.
6. Kornyshev, A. A., and S. Leikin. 1997. Theory of interaction between helical molecules. J Chem Phys 107:3656-3674.
7. Erdélyi, A., W. Magnus, F. Oberhettinger, and F. Tricomi. 1954. Tables of integral transforms. McGraw-Hill New York.
8. Lee, D. J., A. Wynveen, and A. A. Kornyshev. 2004. DNA-DNA interaction beyond the ground state. Phys Rev E 70:051913.
9. Wynveen, A., D. J. Lee, A. A. Kornyshev, and S. Leikin. 2008. Helical coherence of DNA in crystals and solution. Nucleic Acids Res 36:5540-5551.